

# Data-mining Fluoride-Based Solid-State Electrolytes for Monovalent Metal Batteries

Gunyoung Heo,<sup>†</sup> Aloysius Soon,<sup>\*,†,‡</sup> and Taehun Lee<sup>\*,¶,§</sup>

<sup>†</sup>*Department of Materials Science & Engineering, Yonsei University, Seoul 03722,  
Republic of Korea*

<sup>‡</sup>*School of Physics, University of Sydney, Sydney 2006, NSW, Australia*

<sup>¶</sup>*Division of Advanced Materials Engineering, Jeonbuk National University, Jeonju 54896,  
Republic of Korea*

<sup>§</sup>*Hydrogen and Fuel Cell Research Center, Jeonbuk National University, Jeonju, 54896,  
Republic of Korea*

E-mail: aloysius.soon@yonsei.ac.kr; taehun.lee@jbnu.ac.kr

## Figures

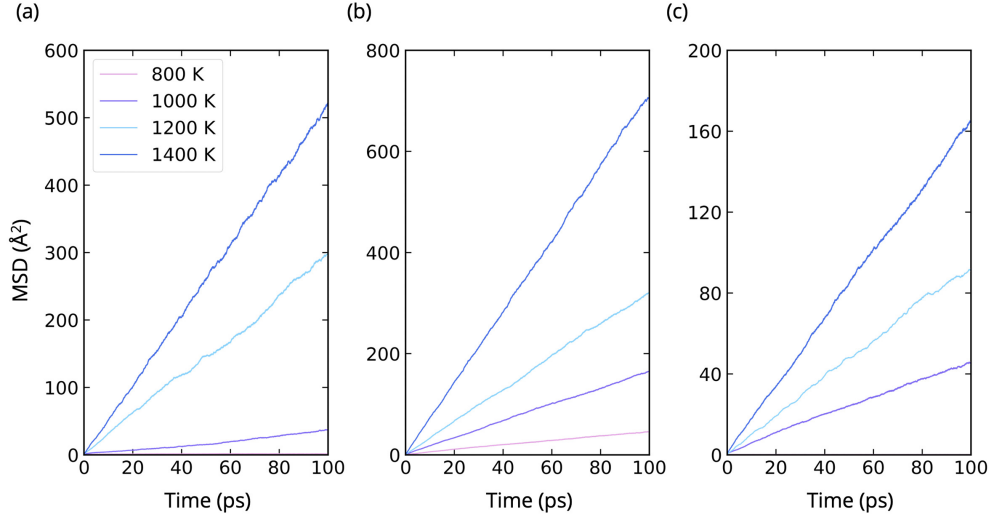


Figure S1: Mean square displacement (MSD) of Li-ion from machine-learned MD simulations over the last 100 ps for Na-based fluorides at various temperatures (800, 1,000, 1,200, and 1,400 K): (a) KLiBeF<sub>4</sub>, (b) Li<sub>3</sub>ScF<sub>6</sub> and (c) NaLiHo<sub>2</sub>F<sub>8</sub>.

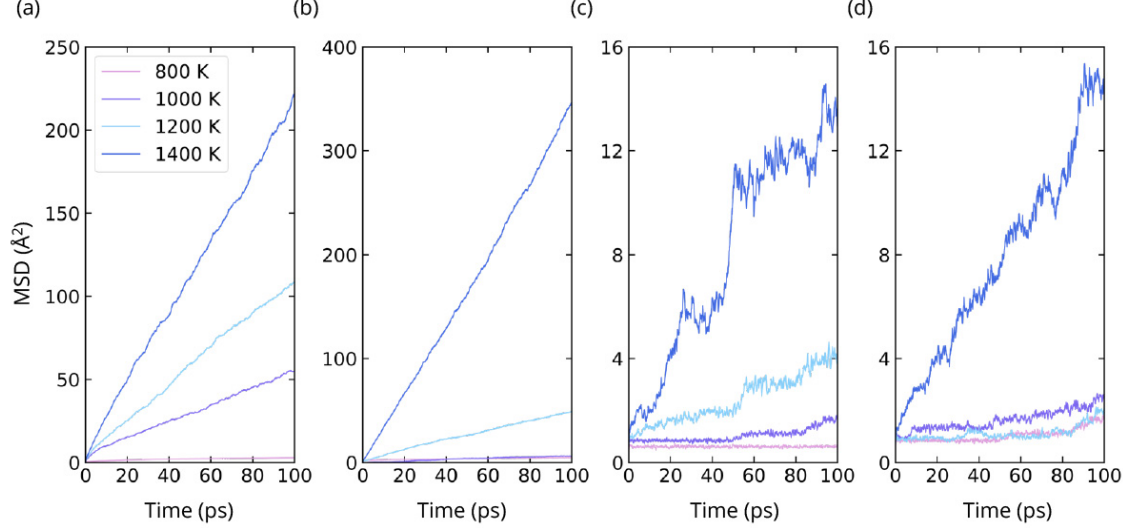


Figure S2: Mean square displacement (MSD) of Na-ion from machine-learned MD simulations over the last 100 ps for Na-based fluorides at various temperatures (800, 1,000, 1,200, and 1,400 K): (a) Na<sub>2</sub>BeF<sub>4</sub>, (b) Na<sub>3</sub>HfF<sub>7</sub>, (c) NaGdF<sub>4</sub>, and (d) NaPrF<sub>4</sub>.

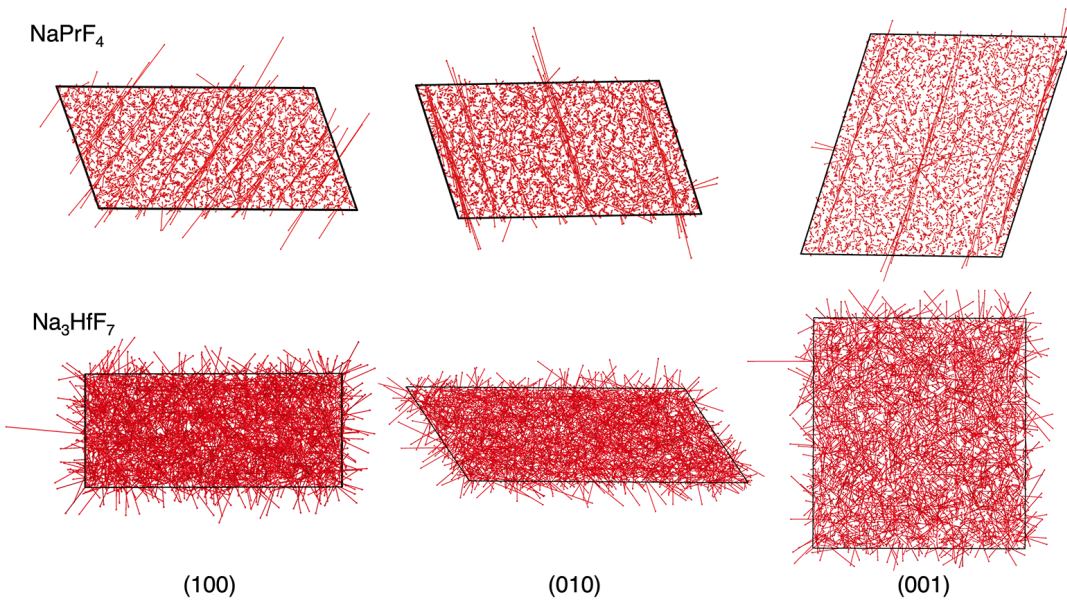


Figure S3: Na-ion diffusion topologies in the supercells of  $\text{NaPrF}_4$  and  $\text{Na}_3\text{HfF}_6$  obtained from the MD trajectory at 1,000 K. The displacement vectors of Na ions are projected with red solid lines within specific crystallographic planes.

## Tables

Table S1: Physiochemical information of Li-based fluoride as the final SSE candidates for LMB obtained through the screening process and MD calculations: compositions, Materials Project-ID (MP-ID), electrochemical stability windows (reduction limit ( $V_{\text{red}}$ ) and oxidation limit ( $V_{\text{ox}}$ )), Pugh ratios ( $P$ ) with their corresponding elastic bulk ( $K$ ) and shear moduli ( $G$ ), and activation barriers ( $E_a$ ) for Li-ion diffusivity for selected candidates which show appreciable ionic diffusion at 1,000 K.

Material	MP-ID	$V_{\text{red}} - V_{\text{ox}}$ (V)	$P$	$K$ (GPa)	$G$ (G Pa)	$E_a$ (eV)
KLiBeF <sub>4</sub>	mp-6253	0.9 – 6.1	1.76	32.45	57.02	1.58
Li <sub>3</sub> ScF <sub>6</sub>	mp-560890	0.4 – 6.2	1.75	39.26	68.75	0.43
NaLiHo <sub>2</sub> F <sub>8</sub>	mp-1210008	0.5 – 6.0	2.46	49.87	122.79	1.51
K <sub>2</sub> LiScF <sub>6</sub>	mp-1111110	0.4 – 6.1	1.91	35.07	67.02	-
LiYF <sub>4</sub>	mp-556472	0.4 – 6.5	1.91	52.22	99.99	-
Rb <sub>2</sub> LiYF <sub>6</sub>	mp-1114432	0.6 – 5.7	2.23	27.97	62.40	-
Rb <sub>2</sub> LiScF <sub>6</sub>	mp-1114702	0.5 – 5.8	2.12	31.60	66.91	-
NaLiEr <sub>2</sub> F <sub>8</sub>	mp-1209986	0.4 – 6.5	2.48	48.80	120.79	-
LiLuF <sub>4</sub>	mp-561430	0.3 – 6.8	2.41	57.34	137.98	-
NaLiLu <sub>2</sub> F <sub>8</sub>	mp-1209991	0.5 – 7.3	2.47	51.63	127.70	-
NaLiTm <sub>2</sub> F <sub>8</sub>	mp-1210006	0.4 – 8.0	2.46	51.14	125.95	-

Table S2: Physiochemical information of Na-based fluoride as the final SSE candidates for NMB obtained through the screening process and MD calculations: compositions, Materials Project-ID (MP-ID), electrochemical stability windows (reduction limit ( $V_{\text{red}}$ ) and oxidation limit ( $V_{\text{ox}}$ )), Pugh ratios ( $P$ ) with their corresponding elastic bulk ( $K$ ) and shear moduli ( $G$ ), and activation barriers ( $E_a$ ) for Na-ion diffusivity for selected candidates which show appreciable ionic diffusion at 1,000 K.

Material	MP-ID	$V_{\text{red}} - V_{\text{ox}}$ (V)	$P$	$K$ (GPa)	$G$ (GPa)	$E_a$ (eV)
NaGdF <sub>4</sub>	mp-1221034	0.1 – 7.1	2.55	46.18	117.94	0.62
Na <sub>2</sub> BeF <sub>4</sub>	mp-3318	0.4 – 6.2	1.81	36.12	65.39	0.77
Na <sub>3</sub> HfF <sub>7</sub>	mp-34579	0.1 – 6.3	2.02	37.21	75.27	0.74
NaPrF <sub>4</sub>	mp-1220948	0.1 – 6.2	2.50	42.78	106.85	0.04
Na <sub>3</sub> ScF <sub>6</sub>	mp-1113433	0.1 – 6.0	1.93	36.29	70.30	-
K <sub>2</sub> NaAlF <sub>6</sub>	mp-6586	0.3 – 6.2	1.98	32.90	65.43	-
Na <sub>2</sub> MgScF <sub>7</sub>	mp-1210466	0.3 – 6.0	1.98	38.48	76.44	-
K <sub>3</sub> NaBe <sub>2</sub> F <sub>8</sub>	mp-1211627	0.4 – 5.8	1.92	30.61	58.95	-
Na <sub>2</sub> ThF <sub>6</sub>	mp-4829	0.2 – 6.0	2.33	38.77	90.64	-
NaYF <sub>4</sub>	mp-1220682	0.1 – 6.1	2.01	44.42	89.39	-
NaHoF <sub>4</sub>	mp-1220708	0.1 – 6.1	2.51	46.00	115.60	-
NaSmF <sub>4</sub>	mp-1220915	0.1 – 6.0	2.48	46.69	116.18	-
NaErF <sub>4</sub>	mp-1221036	0.1 – 6.1	2.51	47.69	119.72	-
NaMgF <sub>3</sub>	mp-2955	0.1 – 6.0	2.02	38.09	77.01	-
Rb <sub>2</sub> NaAlF <sub>6</sub>	mp-1079583	0.3 – 5.8	2.20	29.38	64.77	-
Rb <sub>3</sub> NaBe <sub>2</sub> F <sub>8</sub>	mp-13630	0.3 – 5.5	2.15	26.62	57.37	-
Rb <sub>2</sub> NaErF <sub>6</sub>	mp-13815	0.1 – 5.6	2.63	24.88	65.62	-
K <sub>2</sub> NaScF <sub>6</sub>	mp-6058	0.1 – 5.8	2.01	29.31	59.09	-
Rb <sub>2</sub> NaHoF <sub>6</sub>	mp-15318	0.1 – 5.8	2.63	24.64	65.04	-
NaPaO <sub>3</sub>	mp-865120	0.1 – 4.9	2.03	62.15	126.69	-
NaLiLu <sub>2</sub> F <sub>8</sub>	mp-1209991	0.1 – 6.4	2.47	51.63	127.69	-
NaNd <sub>9</sub> (Si <sub>3</sub> O <sub>13</sub> ) <sub>2</sub>	mp-1221031	0.2 – 4.0	2.08	80.52	167.82	-
NaLiTm <sub>2</sub> F <sub>8</sub>	mp-1210006	0.1 – 8.0	2.46	51.14	125.94	-

Table S3: Calculated Li an Na-ion diffusivity ( $D$ ) in ( $10^{-7}$  cm $^2$  S $^{-1}$ ) of selected candidates for LMB and NMB for each temperature (1,400 K, 1,200 K, 1,000 K, and 800 K).

System	Material	$D_{1400}$	$D_{1200}$	$D_{1000}$	$D_{800}$
LMB	KLiBeF <sub>4</sub>	835.6	505.8	222.3	1.4
LMB	Li <sub>3</sub> ScF <sub>6</sub>	1192.8	535.4	272.0	73.9
LMB	NaLiHo <sub>2</sub> F <sub>8</sub>	346.4	5 .46	2.2	1.8
NMB	NaGdF <sub>4</sub>	9.2	5.8	1.2	0.1
NMB	Na <sub>2</sub> BeF <sub>4</sub>	348.7	177.4	83.8	3.5
NMB	Na <sub>3</sub> HfF <sub>7</sub>	575.1	76.0	6.1	5.3
NMB	NaPrF <sub>4</sub>	22.2	4.27	2.73	2.57

Table S4: Physiochemical information of Li-based archetype and prepared Li-based chlorides (abbreviated as “prepared”) SSE materials for LMB: compositions, Materials Project-ID (MP-ID), electrochemical stability windows (reduction limit ( $V_{\text{red}}$ ) and oxidation limit ( $V_{\text{ox}}$ )), Pugh ratios ( $P$ ) with their corresponding elastic bulk ( $K$ ) and shear moduli ( $G$ ), and activation barriers ( $E_a$ ). The values of  $E_a$  are taken from previous theoretical studies.

Type	Material	MP-ID	$V_{\text{red}} - V_{\text{ox}}$ (V)	$P$	$K$ (GPa)	$G$ (GPa)	$E_a$ (eV)
<i>Archetype</i>	LLZO	mp-6253	0.1 – 3.1	1.57	80.91	127.36	0.61 [ 1 ]
<i>Archetype</i>	$\text{Li}_3\text{PO}_4$	mp-560890	0.7 – 4.1	1.22	72.78	88.80	0.60 [ 2 ]
<i>Prepared</i>	$\text{LiAlCl}_4$	mp-22983	1.6 – 4.4	2.49	12.70	31.66	0.47 [ 3 ]
<i>Prepared</i>	$\text{Li}_3\text{ErCl}_6$	mp-676361	0.8 – 4.2	2.46	19.22	47.19	0.47 [ 4 ]
<i>Prepared</i>	$\text{Li}_3\text{InCl}_6$	mp-676109	2.3 – 4.4	2.45	14.80	36.30	0.34 [ 5 ]

Table S5: Physiochemical information of Na-based archetype and prepared Na-based chlorides (abbreviated as “prepared”) SSE materials for LMB: compositions, Materials Project-ID (MP-ID), electrochemical stability windows (reduction limit ( $V_{\text{red}}$ ) and oxidation limit ( $V_{\text{ox}}$ )), Pugh ratios ( $P$ ) with their corresponding elastic bulk ( $K$ ) and shear moduli ( $G$ ), and activation barriers ( $E_a$ ). The values of  $E_a$  are taken from previous theoretical studies.

Type	Material	MP-ID	$V_{\text{red}} - V_{\text{ox}}$ (V)	$P$	$K$ (GPa)	$G$ (GPa)	$E_a$ (eV)
<i>Archetype</i>	$\text{Na}_3\text{Zr}_2\text{Si}_2\text{PO}_{12}$	mp-1221034	1.2 – 3.3	1.50	63.04	94.78	0.28 [ 6 ]
<i>Archetype</i>	$\text{Na}_3\text{PS}_4$	mp-3318	1.3 – 2.1	1.62	22.65	36.70	0.54 [ 7 ]
<i>Prepared</i>	$\text{NaAlCl}_4$	mp-23363	1.6 – 4.2	2.76	11.33	31.30	0.42 [ 8 ]
<i>Prepared</i>	$\text{Na}_3\text{ErCl}_6$	mp-28542	0.6 – 3.7	2.84	14.17	40.27	0.65 [ 9 ]
<i>Prepared</i>	$\text{Na}_3\text{InCl}_6$	mp-23503	2.2 – 4.0	2.82	10.98	30.96	0.70 [ 10 ]

## References

- (1) Glass-Type Polyamorphism in Li-Garnet Thin Film Solid State Battery Conductors. *Adv. Energy Mater.* **2018**, *8*, 1702265.
- (2) Kuwata, N.; Iwagami, N.; Matsuda, Y.; Tanji, Y.; Kawamura, J. Thin Film Batteries with Li<sub>3</sub>PO<sub>4</sub> Solid Electrolyte Fabricated by Pulsed Laser Deposition. *ECS Trans.* **2009**, *16*, 53.
- (3) Weppner, W.; Huggins, R. Ionic Conductivity of Solid and Liquid LiAlCl<sub>4</sub>. *J. Electrochem. Soc.* **1977**, *124*, 35.
- (4) Schlem, R.; Bernges, T.; Li, C.; Kraft, M. A.; Minafra, N.; Zeier, W. G. Lattice Dynamical Approach for Finding the Lithium Superionic Conductor Li<sub>3</sub>ErIn<sub>6</sub>. *ACS Appl. Energy Mater.* **2020**, *3*, 3684–3691.
- (5) Li, X. et al. Air-Stable Li<sub>3</sub>InCl<sub>6</sub> Electrolyte with High Voltage Compatibility for All-Solid-State Batteries. *Energy Environ. Sci.* **2019**, *12*, 2665–2671.
- (6) Park, H.; Jung, K.; Nezafati, M.; Kim, C.-S.; Kang, B. Sodium Ion Diffusion in Nasicon (Na<sub>3</sub>Zr<sub>2</sub>Si<sub>2</sub>PO<sub>12</sub>) Solid Electrolytes: Effects of Excess Sodium. *ACS Appl. Mater. Interfaces* **2016**, *8*, 27814–27824.
- (7) Zhu, Z.; Chu, I.-H.; Deng, Z.; Ong, S. P. Role of Na<sup>+</sup> Interstitials and Dopants in Enhancing the Na<sup>+</sup> Conductivity of the Cubic Na<sub>3</sub>PS<sub>4</sub> Superionic Conductor. *Chem. Mater.* **2015**, *27*, 8318–8325.
- (8) Park, J.; Son, J. P.; Ko, W.; Kim, J.-S.; Choi, Y.; Kim, H.; Kwak, H.; Seo, D.-H.; Kim, J.; Jung, Y. S. NaAlCl<sub>4</sub>: New Halide Solid Electrolyte for 3 V Stable Cost-Effective All-Solid-State Na-Ion Batteries. *ACS Energy Lett.* **2022**, *7*, 3293–3301.
- (9) Park, D.; Kim, K.; Chun, G. H.; Wood, B. C.; Shim, J. H.; Yu, S. Materials design of

sodium chloride solid electrolytes  $\text{Na}_3\text{MCl}_6$  for all-solid-state sodium-ion batteries. *J. Mater. Chem. A* **2021**, *9*, 23037–23045.

- (10) Zhao, T.; Kraft, M. A.; Zeier, W. G. Synthesis-Controlled Polymorphism and Anion Solubility in the Sodium-Ion Conductor  $\text{Na}_3\text{InCl}_{6-x}\text{Br}_x$  ( $0 \leq x \leq 2$ ). *Inorg. Chem.* **2023**, *62*, 11737–11745.